Pergamon

Cement and Concrete Research 29 (1999) 1181–1188

CEMENT AND CONCRETE RESEARCH

Aspects of concrete porosity revisited

Sidney Diamond*

Purdue University, School of Civil Engineering, 1284 Civil Engineering Bldg., West Lafayette, IN 47907, USA

Received 26 August 1998; accepted 27 May 1999

Abstract

Aspects of the pore structure of conventional concrete are reviewed. The appearance and distribution of pores are illustrated in the context of the microstructure of normal concretes as viewed in backscatter mode scanning electron microscopy. A significant portion of at least the larger pores found in concrete is considered to be derived from the hollow shell (Hadley grain) hydration mechanism. These pores therefore do not represent remnants of the original space between cement grains, the accepted concept of the origin of "capillary pores." A brief review of the characteristics of surface fractals is provided and experiments are described, indicating that the surfaces constituting the boundaries of at least the larger pores in concrete are fractal in nature, at least over a limited range of self-similarity. It appears that the characteristic fractal dimension describing the pore surfaces is almost constant, regardless of age, water:cement ratio, or most other variables.

Keywords: Cement paste; Microstructure; Image analysis; Pore structure; Hadley grains; Fractal aspects

1. Introduction

It is generally agreed that the pore structure of concrete is one of its most important characteristics and strongly influences both its mechanical behavior and its transport properties. Transport properties are intimately related to the resistance of the concrete to various durability problems. Unfortunately, a number of aspects of the fundamental geometrical and microstructural characteristics of concrete pore structures are imperfectly understood, and comparatively few researchers have addressed the problem.

The present paper represents a further examination of the pore structure of concrete, complementary to that provided in a paper that represented the writer's contribution to the recent Sidney Diamond Symposium [1]. In that paper the writer illustrated the general appearance of pores in concrete as visualized in backscatter scanning electron microscopy (SEM) and discussed certain pore structure characteristics. Evidence was presented that (a) only modest extra pore space is ordinarily found near aggregate grains [i.e., within the cement paste region customarily designated as the interfacial transition zone (ITZ)]; (b) the distribution of pore space within the ITZ is not a smooth radial function of distance from the interface but rather resembles the "bulk" paste in that patchy areas of locally extensive porosity are intermingled with areas of locally sparse porosity; (c) despite its continued use for the purpose, mercury intrusion porosimetry (MIP) does not provide even an approximation to the true size distribution of pores in hydrated cement systems; and finally, (d) pores in concrete generally contain pore solutions whose chemistry represents important (and usually neglected) information, especially concerning durability problems.

In the present paper, after providing some indication of the appearance of pores in concrete as visualized in backscatter SEM, a treatment is provided of two lesser-understood aspects of concrete porosity, viz. the pervasiveness of pores derived from hollow shell hydration grains (Hadley grains) in ordinary concrete and the fractal character of concrete pore systems.

2. Concrete pores as visualized in backscatter mode SEM

It seems evident that pores in concrete need to be visualized and understood in the context of the overall microstructure of the concrete, rather than as objects in isolation. This leads to some difficulty, as the pores in the hydrated cement paste (hcp) component are small with respect to most of the other microstructural features within concrete. The microstructure of concrete consists obviously of several discrete elements; specifically coarse aggregate and sand grains, residual unhydrated cement particles, and the hcp. The latter

* Corresponding author. Tel.: 765-494-5016; fax: 765-496-1364.
E-mail address: diamond@ecn.purdue.edu (S. Diamond)

0008-8846/99/$ – see front matter
PII: S0008-8846(99)00122-2

is not a single microstructural element but a complex that contains several types of hydrated particles, CH, and pores. Air voids form a special subset of pores with its own characteristics.

SEM images displaying pores as characteristic elements within concrete microstructure need to be presented at a magnification that represents something of a compromise; it needs to be large enough to show the pores and low enough that the relationship between the pores and other microstructural features is apparent. Fig. 1 provides such an image, from a mature 0.50 water/cement (w:c) ratio laboratory mixed plain concrete taken originally at a multiplication of 500×. The lower left portion is part of a sand grain with a bright deposit of calcium hydroxide occupying much of its perimeter; the remainder of the field is hcp, showing several fully hydrated phenograins (cement grains that have hydrated in situ, i.e., "inner product") and a relatively coarse-pored groundmass. This field has been chosen because it provides a particularly clear picture of the pore structure; however, it is not particularly representative of the microstructure of typical concretes. The visible porosity in this area is greater than what is seen in many concretes; most fields at this magnification for mature concretes show a few incompletely hydrated cement grains, and the calcium hydroxide deposit depicted here is found on many (but not all) sand and coarse aggregate grains and often occupies only a portion of the perimeter of the grains on which it occurs.

Fig. 2, taken from a different w:c 0.50 concrete, presents a perhaps more typical microstructural assemblage. The visible pore content in the hcp is smaller, the calcium hydroxide layer deposited on the aggregate surface is thinner and less complete, and several partly unhydrated cement grains are visible as very bright areas in the upper portion of the figure.

Casual inspection of the sizes of the pores visible in Figs. 1 and 2 indicates that they range in size up to about 15 μm. This is much larger than the perhaps 0.1-μm upper limit of pore size that would be indicated for this concrete by MIP, as indicated previously [1].

It is usually assumed that the pores large enough to be observed in backscatter mode SEM are "capillary" pores as classically defined. The customary picture is summarized, for example, by Neville [2]: "At any stage of hydration the hardened paste consists of gel, of crystals of $Ca(OH)_2$, some minor components, unhydrated cement, and *the residue of the water-filled spaces in the fresh paste.* These voids are called capillary pores, but within the gel itself, there exist interstitial voids called gel pores. . . . There are thus, in hydrated paste, two distinct classes of pores."

Thus pores in concrete larger than gel pores are conceived to be subdivided remnants of space that existed between cement grains in the fresh concrete at the time of set. Escadiellas and Maso [3] have elegantly imaged such space by quickly freezing pastes and mortars after mixing, evaporating the water, impregnating with resin, and preparing polished specimens for SEM examination. Their figures do indeed show the expected continuous phase space surrounding and separating the individual cement grains.

However, close examination of the pores visible in Figs. 1 and 2, and generally in concrete microstructures, suggest that two classes of pore geometry coexist. Some of the pores are elongated and irregularly and highly convoluted in outline. Others are triangular or ovoid in outline, and are bounded by a definite rim, consisting of a narrow thickness of C-S-H. It would appear reasonable that the irregular, convoluted porosity may be directly inherited from original water-filled space. It is rather more difficult to see how the regular ovoid or triangular pores enclosed within rims can be direct descendants of a continuous fluid phase.

In fact, long neglected findings point to the conclusion that the regular enclosed pores imaged in these figures are

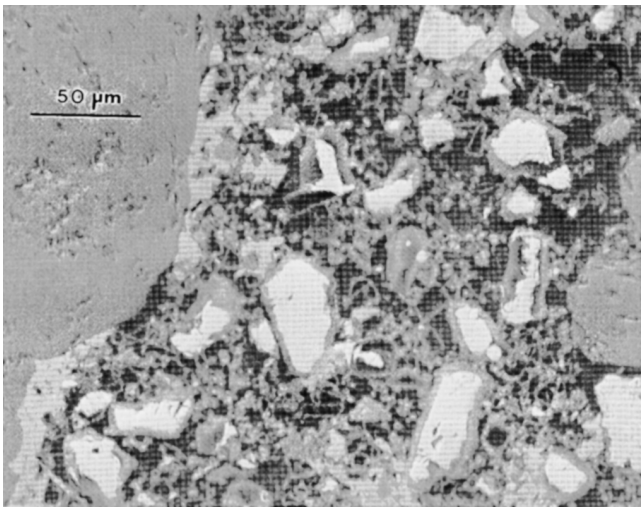

Fig. 1. Backscatter SEM micrograph of laboratory-mixed, 100-day-old w:c 0.50 concrete, selected to show hcp pore system in the context of the concrete microstructure.

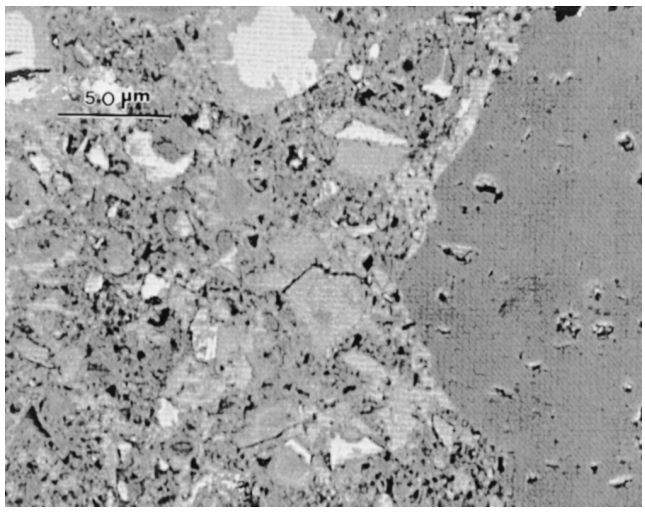

Fig. 2. Backscatter SEM micrograph of a different laboratory-mixed, 100-day-old w:c 0.50 concrete, selected to show a field more typical of concrete microstructure in general.

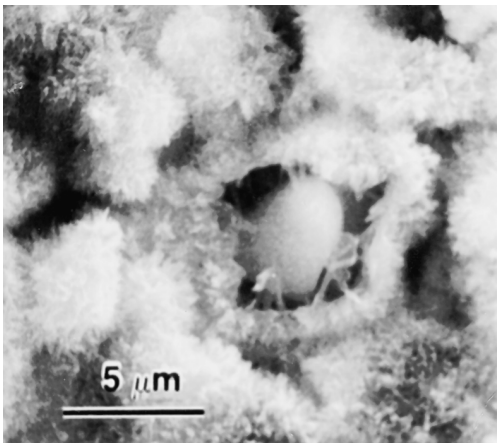

Fig. 3. The original Hadley grain; a reproduction of Fig. 13 from the Ph.D. thesis of D. W. Hadley [4].

not "capillary pores" at all, but rather pore space generated by hollow shell hydration of Hadley grains. Such pores represent space whose origin is within, rather than between, the original cement grains.

3. Evidence for pores derived from hollow shell hydration

In 1972 David W. Hadley completed his seminal thesis at Purdue University on the nature of the paste-aggregate interface in concrete [4]. Working with secondary SEM techniques available at the time, Hadley studied cement paste films deposited on various substrates and then removed from these substrates by fracture induced by drying shrinkage. He noted that occasionally the hydration shell around an individual cement grain was broken in the fracture process, and of such grains, a significant proportion were clearly hydrating by a mechanism involving a hollowing out process, leaving a partly (or eventually completely) hollowed out shell. Fig. 3 is a reproduction of Fig. 13 of Hadley's thesis, taken after 1 day of hydration.

Hadley's work was restricted to simulated paste aggregate interfaces. In his later (1975) thesis at Purdue University, Bobby D. Barnes [5] showed by careful examination that hollow shell hydration grains were not confined to interfacial regions, but were found to occur extensively in bulk cement pastes and mortars, including samples prepared from all of the five existing ASTM cement types except Type IV, which is generally unavailable. The conclusion that hollow shell hydration grains were general in pastes and concretes prepared from a wide range of cements was published by Barnes et al. [6] in 1978.

Fig. 4 show the early stage of the formation of a hollow shell, with a thin shell separated by a 1- to 2-mm gap around a hydrating cement grain. Fig. 5 shows a slightly more advanced stage, with a somewhat thicker shell.

The visualization of the hollow spaces developing within some hydrating cement grains was very much a hit-or-miss affair as long as SEM specimens were prepared by fracturing pastes or concretes. This was a necessary feature in studies using secondary mode SEM. The only way the interior of a particular grain could be visualized was if that grain happened to be accidentally cleaved by the fracture process in the sample preparation. More recently, the development of backscatter mode detectors permits visualization of specimens exposed by slicing and polishing arbitrary plane surfaces, usually of epoxy-impregnated pastes or concretes. As seen in Figs. 1 and 2, this mode of examination provides a cross-sectional view through all of the structural elements present, including the hydrating cement grains; this is a much more satisfactory procedure for most purposes. Unfortunately, the magnification usually obtainable with this technique is limited to about 2,000×. Thus the level of fine detail available, for example, in Fig. 5 (a secondary electron image from a fracture surface) cannot ordinarily be seen in backscatter mode SEM examination.

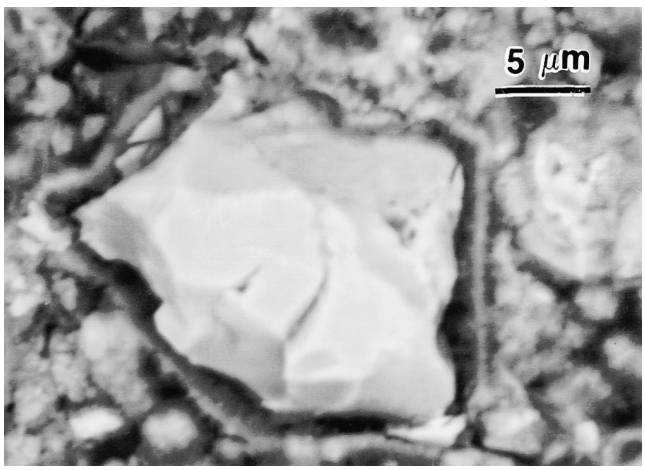

Fig. 4. Secondary electron SEM micrograph depicting the early stage of hollow shell hydration with a thin shell being generated; taken from a 1-day-old w:c 0.50 paste.

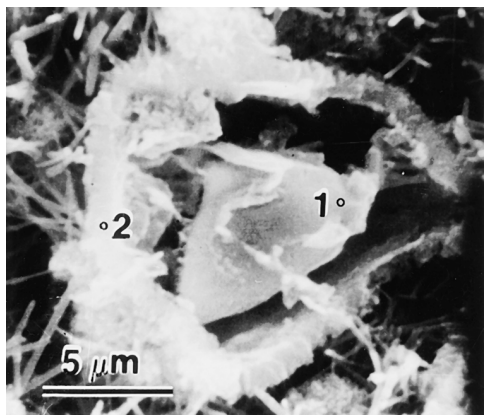

Fig. 5. Secondary electron SEM micrograph showing the early stage of hollow shell hydration with a somewhat thicker shell being generated.

Examination of many hollow shell grains over the years has indicated that many of them, especially in mature concretes, are fully hydrated and remain completely hollowed out. This was noted originally by Hadley [4], who indicated that "by 28 days many of the hydration shells are completely hollow." Close examination of Fig. 2, for example, shows that most of the individual pores of ovoid to triangular shape described earlier appear to represent completely empty hollow shell grains. There are also a few hollow shell grains with residual cores of unhydrated material.

Fig. 6 is an attempt to show the nature of the hollow shell formation process as part of the normal development of hydrating cement paste. The specimen is a 3-day old plain w:c 0.50 paste from ASTM Type I cement with a typical composition. There are two partly empty hollow shell grains with bright floating cores of unhydrated material in the upper left portion of the figure, and a larger, much less hollowed out grain in the middle right portion. More important, much of the groundmass structure can be seen to consist of smaller, regular rimmed pores as seen in the earlier figures. Presumably these were derived from much smaller cement grain fragments that hydrate much more quickly than the coarse grains.

Thus it appears that a significant portion of the pores detectable by SEM in this paste and in normal concretes is not capillary pore space by the standard definition, but rather pore space hollowed out of the interior of cement grains by Hadley grain formation.

It would be of great interest to quantify the proportions of the two kinds of pore space. Image analysis techniques can readily isolate, quantify, and size all of the pores that are large enough to be observed, but to the writer's knowledge, no program has yet been written to distinguish hollow shell pore space from capillary pore space of the same size range.

However, in mature silica fume-bearing concrete it is commonly observed that that the sizes of the capillary pores are smaller than usual, and they are further reduced with progressive hydration. Pores derived from hollow shell seem to remain the same size. A typical example is shown in Fig. 7, from a w:b 0.30 paste with 10% silica fume that was hydrated for 100 days.

Kjellsen et al. [7] have taken advantage of this feature to estimate the hollow shell pore content for silica fume-bearing pastes where the bulk of the non-hollow shell pores are below the limit of detection of the image analysis system. In mature pastes of this kind they found that the pore area percent of hollow shell pores, which constituted all of the pores that could be detected, ranged from a few percent to as much as 9% in different mixes.

The role and importance of hollow shell hydration in ordinary concrete has been little acknowledged over the years. Indeed, even acceptance that the hollow shell mode of hydration exists has been grudging. The writer trusts that this feature of the pore structure of concrete will become more generally appreciated in the future.

4. Explorations of the fractal character of concrete pore systems

The concepts underlying fractal geometry, developed originally by Mandelbrot [8] have now been shown to have application in many fields of research. A number of books on the applications of these concepts have appeared, among them one by Russ devoted specifically to fractal surfaces [9]. In his preface, Russ indicated that despite some abuses, as a phenomenological description of surface geometry, the fractal approach "works" in a surprising number of instances. He considered that "Since this is the way Nature has chosen to behave, it will be important for researchers to apply the new methods of characterization."

Russ divided fractal surfaces into three classes: (1) dense objects with fractal surfaces, (2) "mass fractals" that consti-

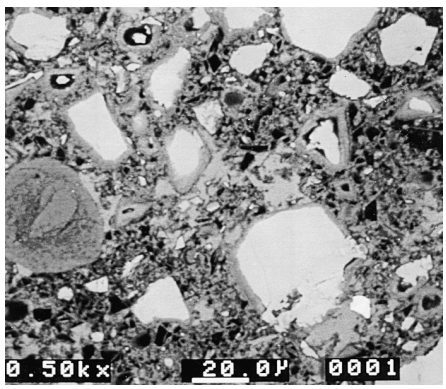

Fig. 6. Backscatter SEM of a large area in a 3-day-old w:c 0.50 concrete, showing the local prevalence of pores derived from hollow shell hydration.

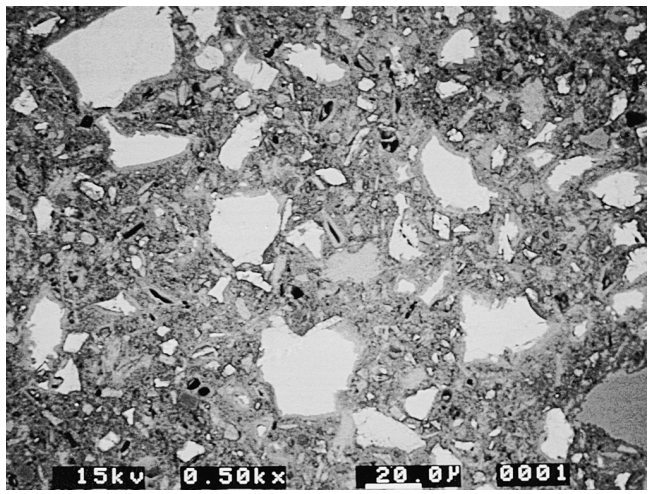

Fig. 7. Backscatter SEM illustrating the microstructure common in mature silica fume pastes, where the only large pores remaining are hollow shell derived pores. The specimen was a w:b 0.30 paste, 10% silica fume, hydrated for 100 days.

tute networks or clusters whose surfaces are also fractal, and (3) pore fractals, defined as dense objects within which there exists a distribution of holes or pores with a fractal structure. If concrete pore structures are fractal, they clearly fall within this third category.

Various methods are available for the characterization of fractal surfaces. These include some that do not deal with the surface in its entirety, but determine its fractal character by working in a lower dimension, that is to say, by studying the intersection of the surface or surfaces with an arbitrary plane. With respect to pores in concrete, working with the two-dimensional pore boundary structure as it is found at the intersection with a plane surface is much more feasible than attempting to work in three dimensions. This is precisely the geometry inherent in backscatter SEM investigation, which would seem to be well suited to the task. Furthermore, since the pores are small, the magnification inherent in SEM is required to properly examination the pore boundaries.

The background underlying the concepts used for measuring the fractal characteristics of boundary lines on a surface derives mostly from the work of Richardson [10], who studied cartographic boundaries on map surfaces. Since comparatively few readers of this journal may be expected to be completely familiar with this work, a brief exposition is provided here, patterned after that provided by Russ [9].

Richardson found that the length of the land-sea boundary between two points on the geometrically irregular west coast of Britain depended on the scale at which the measurement was accomplished. Repeated measurements were made by "walking" the irregular boundary using a pair of dividers set to various "stride lengths" (i.e., the stride length defining the measurement scale). Using a smaller stride length (i.e., feet instead of miles) always produced a larger value for the total length of the boundary. Richardson found that when the logarithm of the total boundary length was plotted against the logarithm of the stride length used (the "Richardson plot"), a straight line with a negative slope was always generated. The characteristic equation developed is shown in Eq. (1):

$$L = L_o E^{-(DF - D)} \tag{1}$$

where L is the boundary length at a given stride length, L_o is a constant, E is the stride length, D_F is the fractal dimension, and D is the topological dimension of the boundary studied (1 if the boundary is a boundary line on a two-dimensional surface. For such a case the fractal dimension is normally 1 + a fractional component, i.e. is between 1 and 2.

A corresponding equation can be written for a fractal surface boundary in three-dimensional space. Here the topological dimension is 2, and the fractal dimension of a boundary surface in three-dimensional space is normally between 2 and 3.

In applications such as the present one, the value of D_F is directly determined by the sum of the absolute value of the slope of the log-log plot and the 1.00 topological dimension of a line. The same slope is added to 2.00 to generate the "real" fractal dimension D_F of the pore surface boundaries in three-dimensional space.

The higher the fractional part of the fractal dimension, the greater the visual appearance of the roughness of the boundary. Fig. 8, after Russ [9], provides several illustrations of the roughness characteristic of boundaries between 1 and 1.23.

However, the fractal dimension is not primarily a measure of roughness at any particular magnification. The all-important feature of the analysis reflects the fact that the real boundary is composed of irregularities at *all* magnifications pertinent to the range of scale lengths covered (i.e., the increase in observed boundary length with reduction in measuring scale length is the same at any degree of magnification). Thus the boundary is said to be self-similar. In consequence, given an image of the boundary without any scale marking (such as those of Fig. 8), the visual appearance of the roughness gives no clue as to the magnification of the image. In principle, the roughness shown for any fractal dimension in Fig. 8 might describe the rough coastline of an island in miles or a small portion of the same coastline in feet.

This self-similarity is the hallmark of a fractal boundary or surface. The fact that it occurs often in nature would not have been predicted prior to the development of methods of fractal analysis and their application to real systems.

However, boundaries on real objects cannot be self-similar over an infinite range of measurement scales. At some

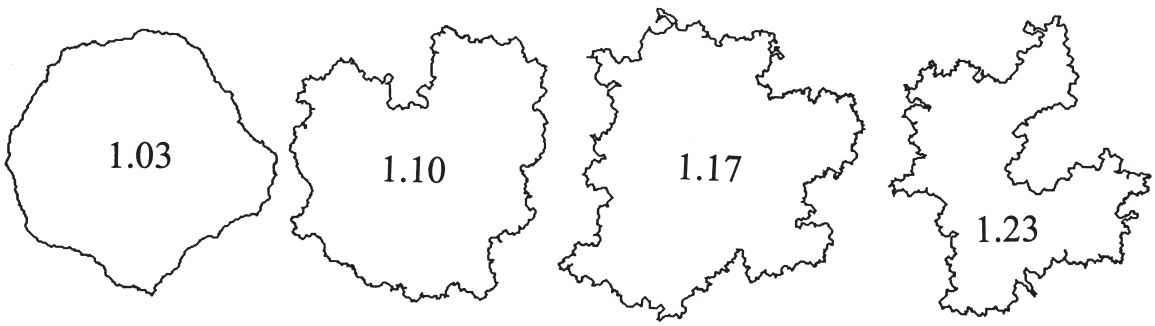

Fig. 8. Illustration of the visual appearance of the roughness of boundaries of fractal objects showing fractal dimensions between 1.00 and 1.23 (after Russ [9]).

large value the measurement scale becomes almost as large or larger than the object; at some sufficiently small value of measurement scale, the experimental resolution used in the measurement is no longer adequate. Either case terminates the self-similarity. An important element of the fractal measurement of a real boundary is the measurement scale range over which the characteristic fractal dimension has been established.

There is one additional important concept. Often, Richardson plots of real boundaries do not follow the ideal behavior outlined above, but instead show two straight line segments of different slopes, with the slope over the scales of smaller length being commonly smaller (less negative) than that over the scales of larger length. These instances have been defined as "mixed fractals"; their widespread occurrence has been extensively documented by Kaye [11] and others. The phenomenon may arise from mixing together two different fractal systems, for example assemblages of particles of two different surface fractal characteristics. More complicated explanations may be required for some systems when mixed fractals are found. In any case, the measurement scale size value at which the transition occurs is another item of significant information derived from the measurement.

In experiments carried out several years ago at Purdue University, Wang [12] investigated the fractal characteristics of pores in hardened cement paste. The analysis was carried out on pore boundaries intersecting a plane of observation, the plane being that of the polished surface of a backscatter SEM specimen. For the analysis Wang used one of the classical approaches for measurement of fractal dimensions of boundaries on a surface, the boundary dilation technique developed originally by Flook [13].

Wang's measurements involved the following steps: (1) digital capture of the backscatter SEM image of an area on the prepared surface of a cement paste at high resolution; (2) a binary segmentation that removed all features except the pores; (3) removal of the smallest pores (less than 0.25 μm) by hole filling; (4) accurately imaging the boundary outlining all of the remaining pores by first eroding a single pixel depth and then subtracting the eroded image from the original image; (5) progressively dilating the single pixel depth boundary in a series of steps of increasing numbers of layers of pixels; and (6) measuring the perimeter length at each stage of dilation. As seen in Fig. 9, the successive dilation steps simulate a progressive reduction in resolution; more and more boundary details disappear with each dilation step. Thus the extent of dilation serves as the characteristic measurement scale of the analysis.

In this work cement pastes were prepared at w:c ratios of 0.30 and 0.45 and hydrated for 3 or 100 days prior to examination. In addition to plain pastes, pastes mixed with superplasticizer, silica fume, and the combination of the two were also examined.

All of the images examined were high resolution images secured at 2,000× at 1024 × 1024 pixel resolution. The pixel size was 0.06 μm and dilation took place in eight steps.

The results of this analysis indicated that for all pastes examined, the pore systems were fractal over the entire measuring scale range examined, from 0.06 μm to slightly over 1 μm. This measuring scale range should not be confused with the size range of the pores examined in the analysis, which varied between 0.25 μm and the largest pore present in a given field, typically about 15 μm.

A Richardson plot typical of the data obtained is shown in Fig. 10. As is evident from the figure, the relationship found was characteristic of mixed fractals. The transition between the two fractal regimes was typically found at a measuring scale length of about 0.4 μm.

The fractal dimensions corresponding to the two portions were 1.1 for the smaller scale length portion and 1.3 for the larger scale length portion. These are boundary fractal numbers describing the pore boundaries on the surface imaged. The corresponding pore surface fractal dimensions in space are 2.1 and 2.3, respectively.

Wang [12] found little variation with age or with w:c ratio. All of the pore systems examined showed mixed fractals of roughly the same fractal dimensions. About the only meaningful variation was that found with superplasticized pastes, which showed rather higher fractal dimensions for larger scale length portion, approaching 1.5 for the pore boundary fractal. Wang noted that the pores in these superplasticized pastes showed a much more intricate and convoluted appearance in the SEM.

It is tempting to speculate that the mixed fractal character of the pore systems found by Wang is a consequence of the occurrence of the two different classes of pore geometry indicated previously, with the more convoluted true capillary pores being responsible for the higher fractal dimension and the more regular Hadley grain pores being responsible for the lower fractal dimension. However, such a conclusion is premature for several reasons.

One of them is that Lange et al. [14] report somewhat different results from a similar study carried out on several cement pastes and mortars. Their images were obtained at somewhat lower resolution, their procedures were somewhat different from those of Wang, and their analyses was deliberately confined to only the largest sized pores present. Lange et al. found that all of the pore systems examined were indeed fractal, but they found no indication of mixed fractal character. The fractal dimension found was universally 1.25 in pore boundary fractal terms (i.e., between the two separate fractal dimensions found for the mixed fractals detected in Wang's work).

Despite the discrepancy, the fractal character of the surfaces of the larger pores in cement paste and concrete can be considered to be well established, along with the approximate magnitude of the fractal dimension and the fact that there is very little variation with age, w:c ratio, and other characteristics of the material. The full significance of these findings await further study.

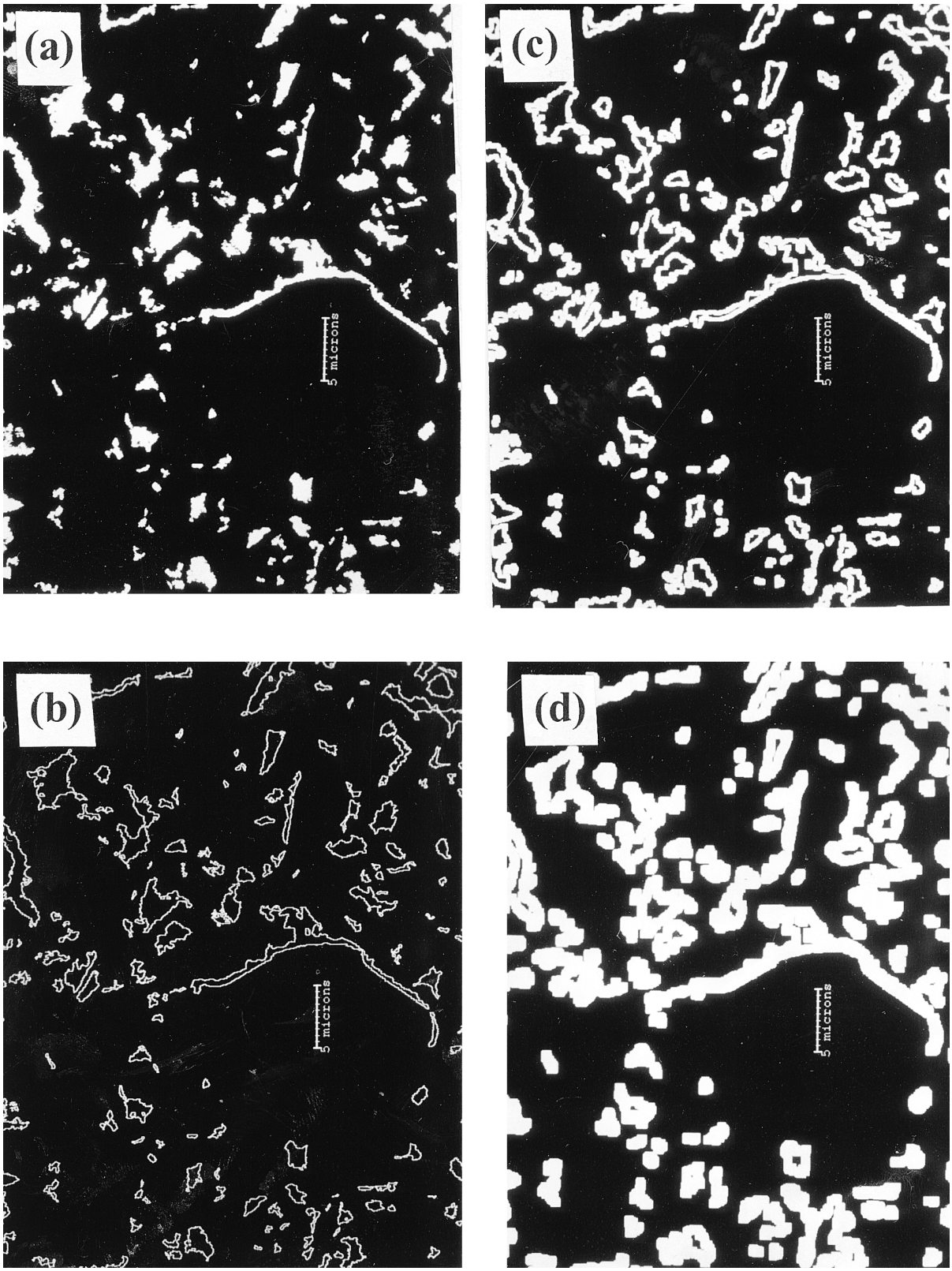

Fig. 9. Illustration of the effects of progressive dilation on the outline of pores in hcp: (a) original segmented pore image, (b) single-pixel thick outline, (c) outline after two dilation steps, and (d) outline after five dilation steps (after Wang [12]).

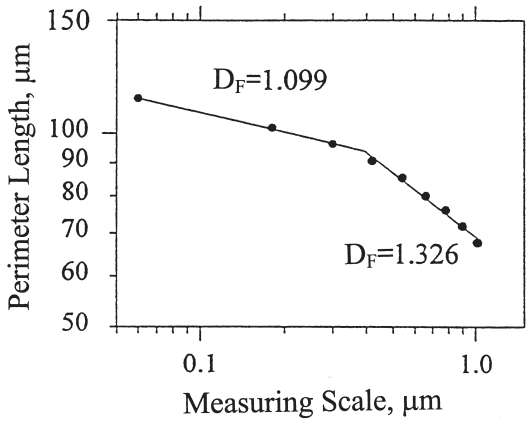

Fig. 10. Typical Richardson plot for hcp pore outlines exposed to the progressive dilation method of fractal analysis (after Wang [12]).

Acknowledgments

The writer is indebted to the late David W. Hadley, Bobby D. Barnes, and Yuting Wang, who provided the primary source of the various items of data discussed in this paper, and to Jingdong Huang. Continuing research support by the National Science Foundation Center for Advanced Cement-Based Materials is gratefully acknowledged.

References

[1] S. Diamond, Concrete porosity revisited, in: M.D. Cohen, S. Mindess, J. Skalny (Eds.), Materials Science of Concrete: Special Volume—The Sidney Diamond Symposium. American Ceramic Society, Westerville, OH, 1998.
[2] A. Neville, Properties of Concrete, 4th ed., John Wiley and Sons, Inc., New York, 1996, p. 25.
[3] G.C. Escadiellas, J.C. Maso, Approach of the initial state in cement paste, mortar, and concrete, in: S. Mindess (Ed.), Advances in Cementitious Materials, Ceramic Transactions Vol. 16, American Ceramic Society, Westerville, OH, 1991, pp. 169–184.
[4] D.W. Hadley, The nature of the paste-aggregate interface, Ph. D. thesis, Purdue University, 1972.
[5] B.D. Barnes, Morphology of the paste-aggregate interface, Ph.D. thesis, Purdue University, 1975.
[6] B.D. Barnes, S. Diamond, W.L. Dolch, Cem Concr Res 8 (1978) 263.
[7] K.O. Kjellsen, B. Lagerblad, H.M. Jennings, J Matls Sci 32 (1977) 2924.
[8] B.B. Mandelbrot, The Fractal Geometry of Nature, Freeman Publishers, New York, 1982.
[9] J.C. Russ, Fractal Surfaces, Plenum Press, New York, 1992.
[10] L.F. Richardson, The Problem of Contiguity: An Appendix of Statistics of Deadly Quarrels, General Systems Yearbook, Vol. 6, 1961, pp. 139–187.
[11] B.H. Kaye, A Random Walk Through Fractal Dimensions, VCH Verlagsgesselchaft, Weinheim, Germany, 1989.
[12] Y. Wang, Microstructural study of hardened cement paste by backscatter scanning electron microscopy and image analysis, Ph. D. thesis, Purdue University, 1995.
[13] A. Flook, Powder Technol 21 (1978) 295.
[14] D. Lange, H.M. Jennings, S.P. Shah, Cem Concr Res 24 (1994) 841.